Epoxidized natural rubber-50 toughened polyamide 6 nanocomposites: The effect of epoxidized natural rubber-50 contents on morphological characterization, mechanical and thermal properties

**Hamed Nouparvar[1], Azman Hassan[1],
Zurina Mohamad[1] and Mat Uzir Wahit[1]**

Abstract

Nanocomposites consisting of polyamide 6 (PA6) matrix with epoxidized natural rubber 50 (ENR-50) and organoclay-modified montmorillonite was prepared by melt blending in a twin-screw extruder followed by injection molding. The influence of varying amounts (0–30 phr) of ENR-50 loadings on ENR-50-toughened PA6 nanocomposites was examined. Morphological characterizations and mechanical and thermal properties of the blend and nanocomposites were investigated. Addition of ENR-50 resulted in a decrease in the tensile strength and modulus, while impact strength enhanced until a maximum at 10 wt% ENR-50. Thermal study revealed no significant change in the thermal properties with ENR-50 loadings. Exfoliated structure was observed using the x-ray diffraction patterns and was confirmed by transmission electron microscopic

[1] Department of Polymer Engineering, Faculty of Chemical Engineering, Universiti Teknologi Malaysia, Skudai, Johor, Malaysia

Corresponding author:
Azman Hassan, Department of Polymer Engineering, Faculty of Chemical Engineering, Universiti Teknologi Malaysia, 81310 Skudai, Johor, Malaysia.
Email: azmanh@cheme.utm.my

images. Scanning electron microscopic images revealed dispersed ENR-50 particles and increased rubber particles size with increasing ENR-50 loadings.

Keywords

Introduction

Polymer nanocomposites refer to composites where one of the components has at least one dimension of the order of a few nanometers. Some types of inorganic materials such as fiber glass, calcium carbonate, talc and clay minerals have been successfully used as additives or reinforcement to enhance strength and stiffness of polymer matrix. Polymer nanocomposites based on layered silicates have been developed to overcome the disadvantages of conventional additive such as glass fiber-reinforced polymers. These have inferior surface quality, increased density and loss of transparency. Compared with macro- and microfillers, these nanocomposites exhibit superior properties such as enhanced mechanical properties, improved flame retardancy and barrier properties as well as heat resistance. The enhanced properties of polymer nanocomposites are presumably due to the formation of nanoscale structure, large aspect ratio, large area of the layered silicates and strong interaction between polymer molecular chains and layered silicates.[1–5]

Polyamide 6 (PA6) is an excellent polar thermoplastic polymer with regards to its attractive combination of inexpensive and amazing versatility in terms of properties and applications such as electronic industries, medical and health applications, food packaging, and automotive industry.[1–3] Furthermore, PA6 has amine and carboxyl functional groups,[6,7] which interacts with many substances such as fillers,[8,9] impact modifiers[10,11] and flame retardants[12,13] for new applications.

Numerous research described PA6/organoclay nanocomposites to exhibit high modulus, high distortion temperature and good barrier properties of gas and water.[1–3] Russo et al.,[14] revealed that the technological relevance of nylon 6-layered silicate nanocomposites is declared by many patents issued over the last few years which highlight the significant increases in the structural and functional properties with the addition of very low organoclay content, usually less than 5 wt%. Tensile modulus and strength were found to increase with increasing concentration of clay.[15] The property improvements are attributed to the high stiffness and strength of the clay particles and the interaction of the polymer chains with the exfoliated clay lamellae.[5] Conversely, the impact strength and elongation at break decrease in the presence of organoclay loading.[16,17] In addition, the nanocomposites are more brittle and notch sensitive to crack propagation than pure PA6 at room or lower temperature.[18]

Some drawbacks such as brittleness and notch sensitive to crack propagation at ambient or lower temperature of PA6/organoclay limit its application. Numerous research have been carried out on the improvement of these properties.[19] Rubber-toughened plastics constitute a commercially important class of polymers, which are characterized by a

combination of fracture resistance and stiffness.[20] It is recognized that the toughening of PA6/organoclay can be achieved by incorporating a low-modulus second component.[21] The philosophy behind this approach is to produce polymer nanocomposite systems that possess a good balance in stiffness, strength and toughness.[19,22] Incorporation of rubber achieved toughness but resulted in reduced tensile strength and modulus. Compounding with organoclay enhances modulus and stiffness but decreases toughness. Many researchers have published articles on PA6 or PA6/MMT nanocomposites toughened by various types of rubbers to improve impact properties of the nanocomposites. For example, common impact modifiers used are ethylene propylene diene monomer (EPDM-*g*-MA),[19,22] ethylene propylene rubber (EPR),[11,23] maleated polyethylene-octene (POE-*g*-MA)[24] and styrene-(ethylene-co-butylene)-styrene (SEBS).[25,26]

Epoxidation of natural rubber (NR) was first conducted in 1922 by Pummerer and Bukhard, but the potential applications of epoxidized natural rubber (ENR) were only realized in the 1980s.[27] NR displays high mechanical strength, outstanding resilience and excellent elasticity. However, NR is known to have poor wet grip properties and poor weather resistance.[27] ENR is now an established commercial rubber polymer, which is produced by the chemical modification of NR. They have a unique set of properties offering high strength, due to their ability to undergo strain crystallization, along with increased glass transition temperature and solubility parameters. These properties are reflected with increased oil resistance, enhanced adhesion properties, high degree of damping and reduce gas permeation.[28] ENR was selected due to its high polarity, which should be beneficial when compounding with polar fillers, such as layered silicates.[29] The functional group interactions also result in ENR forming compatible blend with a range of polymers.[28] When ENR-50 is used, its epoxy-containing groups can react with the nylon 6 matrix forming graft copolymer, ENR-50-*g*-PA6.[30] Nematzadeh et al.[31] studied the mechanical and thermal properties of ENR-25 toughened PA6 nanocomposites at different contents of ENR-25. The morphological properties of ENR-50-toughened PA6 nanocomposites are not yet reported.

The aim of the current research is to investigate the properties of ENR-50-toughened PA6 nanocomposites. These nanocomposites (thermoplastics/nanofillers) often show amazing improvement in the material properties compared with virgin polymer and microcomposites. In addition, PA6/organoclay-modified montmorillonite (OMMT) nanocomposite is brittle and notch sensitive; therefore, toughening of PA6/OMMT is necessary to improve the properties of the nanocomposites. Thus, the need to achieve new formulation for ENR-50-toughened PA6 nanocomposites by adding ENR-50 as an impact modifier is necessary. In view of above, the investigation of the effect of ENR-50 concentration on mechanical and thermal properties and the morphological characterization of ENR-50 toughened PA6 nanocomposites were carried out.

Experimental

Materials

The PA6 (Amilan CM 1017) was a commercial product from Toray Nylon Resin (Amilan, Japan). The melt flow index of PA6 was 35 g/10 min at 230°C and 2.16 kg

Table 1. Materials designation and compositions.

	Composition		
Designation	PA6 (wt%)	OMMT (phr)	ENR-50 (wt%)
PA6/F4	100	4	–
PA6/F4/E10	90	4	10
PA6/F4/E20	80	4	20
PA6/F4/E30	70	4	30

PA6: polyamide 6; ENR: epoxidized natural rubber; OMMT: organoclay-modified montmorillonite.

(21.2 N), and the density was 1.14 g/cm^3. The ENR-50 with 50 mol% epoxidation was produced by the Malaysian Rubber Board, Malaysia. The organoclay (Nanomer 1.30 TC) was a commercial product from Nanocor Inc. (Arlington Height, Illinois, USA). It was a white powder containing montmorillonite (70 wt%) intercalated by octadecyla-mine (30 wt%) suitable for the use in PA6 matrix.

Compounding and test specimen preparation

Prior to melt blending, PA6 pellets were dried for 24 h at 82°C in a vacuum oven to avoid moisture-induced degradation reactions. ENR-50 was masticated using two-roll mill then cut into small pieces. The polymers and additives were then melt blended by the simultaneous addition of all the components into a Brabender 2000 (Germany) corotating twin screw extruder. The compound formulations are shown in Table 1. The barrel temperatures were gradually increased from hopper to die at 200, 220, 230 and 240°C and the rotating screw was 50 r/min. The pelletized materials were dried for 8 h at 82°C and injection molded into shapes required for standard tensile, flexural and impact specimens using a JSW (Muroran, Japan) Model N100B II injection molding machine with a barrel temperature of 210–240°C. All the specimens were kept under ambient conditions in a desiccator at least 24 h prior to testing.

Mechanical properties

Tensile and flexural tests were carried out according to ASTM D638 and ASTM 790 using an Instron (Bucks, UK) 5567 Universal Testing Machine under ambient conditions. The crosshead speed for tensile testing was 50 mm/min and flexural testing was 3 mm/min. Izod impact tests were carried out on the notched specimens using Toyoseiki (Tokyo, Japan) impact tester under ambient conditions according to ASTM D256. The values reported in this study were the average of five values. The notch depth was 2.6 $\pm$ 0.02 mm.

Thermal analysis

Differential scanning calorimetry. Analysis of the melting and crystallization behavior of the blends and nanocomposites was carried out using a Perkin-Elmer (Boston,

Massachusetts, USA) DSC7 differential scanning calorimeter. All the experiments were carried out under nitrogen atmosphere. All specimens were in the range of 6–10 mg in weight. Samples were heated at 10°C/min from 30 to 280°C and held at the maximum temperature for 1 min. They were then cooled to 30°C and heated for a second time to 280°C at a heating rate of 10°C/min in other to erase the thermal history. The melting temperature (T_m) and crystallization temperature (T_c) were taken as the temperatures corresponding to the peak values of the melting endotherms and exotherms, respectively. The degree of crystallinity (X_c) was calculated as the ratio of the melting enthalpy to the melting enthalpy of 100% crystalline PA6 based on weight fraction of PA6 (w_{PA}) in blend from the following equation[16]

$$X_c(PA6) = \left(\frac{\Delta H}{w_{PA6} \cdot \Delta H^\circ} \right) \times 100 \tag{1}$$

where ΔH is the measured enthalpy of melting, and $\Delta H^\circ = 190.8$ J/g[16] is the melting enthalpy of 100% crystalline PA6.

Thermogravimetric analysis. Thermogravimetric analysis (TGA) was performed with a Perkin-Elmer TGA7 thermal analysis system in order to examine the thermal stability behavior of the organic and inorganic components in the blends. Approximately, 10–15 mg of samples were scanned under nitrogen from 25 to 950°C, at a heating rate of 10°C/min.

Morphological characterization

X-Ray diffraction. X-Ray diffraction (XRD) technique was performed with Siemens (Berlin, Germany) x-ray diffractometer (D5000) in step scan mode using Ni-filtered Cu K radiation (0.1542 nm wavelength) at a generator voltage of 40 kV. The diffraction patterns were recorded with a step size of 0.02° from $2\theta = 2$–10°. The interlayer spacing of the organoclay in the nanocomposites was derived from the peak position (d001-reflection) in XRD scans according to the Bragg's equation[32]

$$n\lambda = 2d \sin\theta \tag{2}$$

where $n = 1$ is an integer, θ is the diffraction angle giving the primary diffraction peak, and $\lambda = 1.54$Å is X-ray wavelength (1nm $= 10$Å).

Scanning electron microscope. The fractured surface morphology of the samples were examined using a Philips (ZL 40) scanning electron microscope (SEM) at an operating voltage of 2.0 kV. Samples were cryogenically fractured in liquid nitrogen and etched in toluene at room temperature for 4 h to extract the elastomeric ENR-50 phase and then the fracture surfaces were coated with gold prior to SEM examination for the rubber particles size and distribution observation.

Transmission electron microscopy. The distribution of OMMT particle characterization was carried out with transmission electron microscopy (TEM; using Model: JEOL
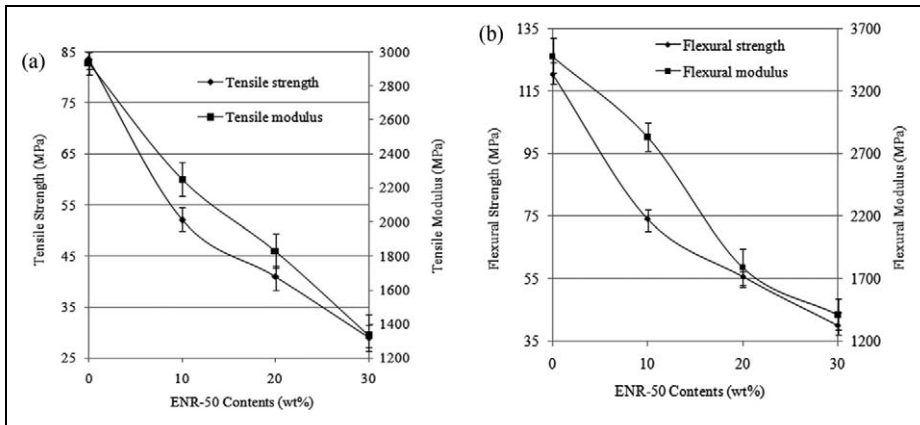
Figure 1. Effect of ENR-50 contents on tensile and flexural properties of PA6 blend and nanocomposites. (a) Tensile strength and tensile modulus and (b) flexural strength and flexural modulus.PA6: polyamide 6; ENR: epoxidized natural rubber.

(JEM-2100)), which was operating at an accelerating voltage of 120 kV. The samples were cryogenically cut into ultrathin sections with a diamond knife of about 30–50 nm thick.

Results and discussion

Mechanical properties

Figure 1(a) shows the effect of ENR-50 contents on tensile strength and modulus of PA6/OMMT nanocomposites. Tensile strength and modulus decreased as ENR-50 content increased from 0 to 30 wt% by about 65% and 54%, respectively, when compared with PA6/OMMT nanocomposite. Similar trends as that of tensile properties were observed for flexural properties. Flexural strength and flexural modulus as the functions of ENR-50 reduced by about 63% and 59%, respectively, with similar increase in ENR-50 concentration as shown in Figure 1(b). These observations are generally found in various polymer nanocomposites and have been reported to be due to the softening or dilution effect of a soft elastomeric phase incorporation into the matrix which increases the chains mobility of PA6 matrix.[31,33] The incorporation of ENR-50 causes the formation of grafted copolymer of PA6-*g*-ENR-50, which facilitates dispersion of ENR-50 into PA6 matrix. Therefore, low T_g and softening nature of ENR-50 due to its low modulus decrease the strength and modulus. The specific interaction via epoxide groups has previously been proposed by Gelling.[28] He proposed that the functional groups' interactions result in ENR forming a compatible blend with a range of polymers. The decrease in strength and modulus of the PA6 with the addition of ENR-50 is consistent with two earlier studies reported by Xie et al.[30] and Tanrattanakul et al.[34]
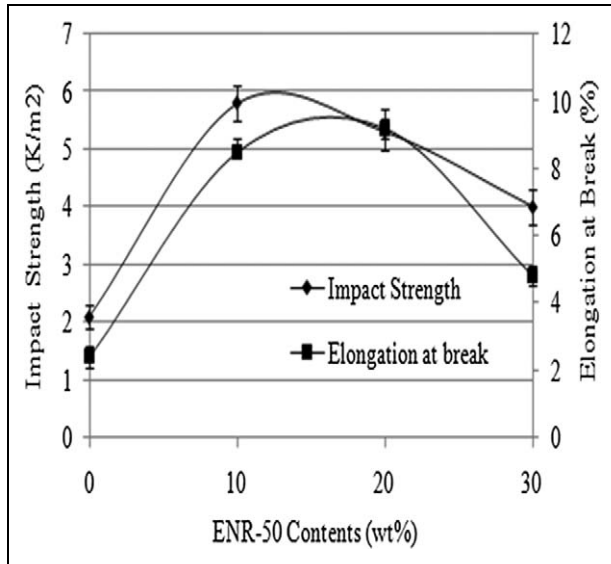
Figure 2. Effect of ENR-50 contents on the elongation at break and impact strength of PA6 blend and nanocomposites. PA6: polyamide 6; ENR: epoxidized natural rubber.

Figure 2 shows PA6/OMMT nanocomposites that are successfully toughened using ENR-50. Impact strength and elongation at break increased by increasing ENR-50 concentration from 0 to 30 wt% ENR-50 in PA6 nanocomposites when compared with PA6/OMMT blend. Interestingly, impact strength significantly improved until it reaches a maximum at 10 wt% ENR-50 by about 177%, while elongation at break shows a significant improvement until it reaches a maximum at 20 wt% ENR-50 by about 254%, when compared with PA6/OMMT blend. The improvement in toughness and elongation at the break of blends with the addition of ENR-50 when compared with PA6/OMMT could be ascribed to several factors such as nature of matrix, ENR-50 concentration, interfacial adhesion between rubber particles and matrix, rubber particle performance (size and shape), blending method and processing conditions. The epoxy groups in ENR-50 have polarity and possibility to chemically react with carboxyl and amine groups of PA6. This improves miscibility and compatibility as well as interface between rubber and PA6 matrix. This results in better distribution of ENR-50 in PA6 matrix and enhances the chains mobility of the polymer matrix. Generally, when force is applied to rubber-toughened nanocomposites, both the matrix and rubber bear the force and try to absorb energy. Therefore, good dispersion of rubber can lead to homogeneous structure and softening that can control crack and cavitation propagation. In another words, high rubber phase dispersion could act as an effective stress concentrator, enhanced both crazing and shear yielding in the matrix. Both the processes are capable of dissipating larger amount of energy, which will then lead to a significant increase in the toughness of the blends. It is proved that an interface between

Table 2. DSC results of PA6 nanocomposites with different ENR-50 contents.

Sample	T_m (°C) γ-form	T_m (°C) α-form	T_c (°C)	X_c (%)
PA6/F4	213.5	220.7	185.4	21.8
PA6/F4/E10	211.7	219.7	183.6	19.6
PA6/F4/E20	210.0	217.2	183.9	18.0
PA6/F4/E30	209.8	216.7	183.4	15.8

PA6: polyamide 6; ENR: epoxidized natural rubber; DSC: differential scanning calorimetry.

ENR-50 and PA6 improved by forming PA6-g-ENR-50 copolymer.[30] Many researchers have explained that the functional group in rubber is believed to react with the terminal groups of PA6, thus improving the distribution of rubber particles in the polymer matrix.[30,34–36] This indicates that the distribution of ENR-50 with low modulus has a significant toughening effect, decreased notch-sensitivity and increases toughness at low temperature. In addition, possible intermolecular attraction between PA6/OMMT and ENR-50/OMMT contributes to improvement in compatibility between substances. This is supported with similar observations by numerous researchers.[30,34,37]

In addition, reduction in impact strength and elongation at break (30% and 43%, respectively) were observed after further addition of ENR-50 up to 30 wt% compared with PA6/F4/E10, which is still higher than PA6/F4 blend. It may be ascribed to rubber agglomeration due to rubber–rubber interactions, which effects on size, shape and aspect ratio of ENR-50 particles in PA6 nanocomposites. This is an indication that the rubber particle size is an important factor in cavitation.[38] Another factor related to upper and lower rubber particle size is critical interparticle distance and interface adhesion between rubber and polymer matrix.[39,40] Souheng[39] considered that only strong adhesion due to interfacial grafting between rubber and nylon is not sufficient for toughening. Besides strong adhesion, the particle size must also be smaller than the critical size to achieve a tough behavior.[39]

Thermal analysis

Differential scanning calorimetry. Table 2 shows differential scanning calorimetric (DSC) scan results of PA6/F4 and ternary PA6 nanocomposites, which summarized the detail results of crystallization temperature (T_c), melting temperature (T_m) and percentage crystallinity (X_c). Two melting peaks can be seen in Table 2; the higher temperature corresponds to the melting point of α-form crystal and the lower peak temperature relates to γ-form crystal.[4,32,41] The α-form is thermodynamically stable but the γ-form is kinetically favored. Furthermore, Xie et al.[30] have reported that ENR-50 is compatible with PA6 and decreased the crystallinity of PA6.

It is obvious (Table 2) that the melting temperature for α- and γ-form decreased by about 2 and 1°C, respectively, upon adding 10 wt% ENR-50 to PA6 nanocomposites. Presumably, the melting temperature reduced due to ENR-50 having good interaction with PA6 and lower T_m of ENR-50 compared with PA6. Addition of ENR-50 (up to 30%) further reduced T_m of the nanocomposites. In addition, Table 2 shows that the

Table 3. TGA results for PA6/ENR-50/OMMT nanocomposites.

Designation	$T_{10\%}$ (°C)	$T_{90\%}$ (°C)
PA6/F4	438	540
PA6/F4/E10	396	477
PA6/F4/E20	390	477
PA6/F4/E30	385	473

PA6: polyamide 6; ENR: epoxidized natural rubber; OMMT: organoclay-modified montmorillonite; TGA: thermogravimetric analysis.

addition of 10 wt% ENR-50 to PA6 nanocomposite (PA6/F4/E10) reduced T_c by about 2°C but remains relatively constant with the further addition of ENR-50. This shows that ENR-50 contents do not significantly influenced T_c. X_c also reduced in the presence of 10 wt% ENR-50 (PA6/F4/E10) when compared with PA6/OMMT. Addition of ENR-50 up to 30 wt% to PA6 nanocomposites shows further reduction in X_c. This implies that ENR-50 reduced X_c of PA6 nanocomposites. This is consistent with a previous study on the effect of ENR-50 on PA6/EPDM blend.[30]

Thermogravimetric analysis. Thermal stability of PA6 nanocomposites with varying (0–30 wt%) ENR-50 contents was studied with TGA. The initial degradation temperature ($T_{10\%}$, taken at 10% weight loss) and final degradation temperature ($T_{90\%}$, taken at 90% weight loss) from TGA thermograms are listed in Table 3. All the samples show single step degradation. Thermal stability of rubber-toughened PA6 nanocomposites at $T_{10\%}$ and $T_{90\%}$ was reduced with an increase in the ENR-50 contents from 0 to 30 wt%. This may be ascribed to the lower thermal stability of ENR-50 (approximately 405°C[42]) that is amorphous as second phase compared with PA6 that is mostly crystalline. These results are consistent with Nematzadeh et al.,[31] who have studied ENR-25 contents.

Morphological characterization

Morphology is a main determinant of the properties of heterogeneous polymer blends. For instance, a large particle size and weak adhesion would result in poor mechanical properties in the blends.[20] To comprehend the change in mechanical properties, particularly, the toughening mechanism in these ternary nanocomposites, it is required to clarify the dispersion and phase morphology of clay and rubber particles in PA6 matrix. Clay can either locate in the rubber particles or separately disperse in PA6 matrix.[19]

X-Ray diffraction. XRD is a widely used technique for characterizing clay dispersibility. The XRD patterns of neat OMMT, binary PA6/F4 and PA6 nanocomposites that include various ENR-50 contents (10, 20 and 30 wt%, respectively) are shown in Figure 3. The characteristic (001) diffraction peak of neat OMMT locates evidently around $2\theta = 4.14°$ (d-spacing: 2.13 nm), but no peaks were observed in the XRD patterns for all PA6 nanocomposites (Figure 3). The absence of basal plane peaks also illustrated delamination and well dispersion of the OMMT particles within the PA6 and ENR-50 consequence formation of an
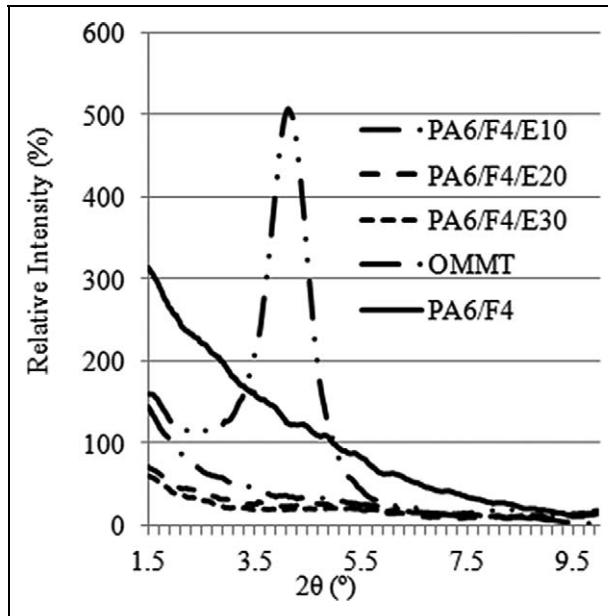
Figure 3. XRD pattern of pure OMMT and PA6 nanocomposites containing different ENR-50 contents. PA6: polyamide 6; ENR: epoxidized natural rubber; XRD: x-ray diffraction; OMMT: organoclay-modified montmorillonite.

exfoliation nanostructure. The increased interlayer distance of organoclay may be the result of the strong interaction between polar PA6 and ENR-50 and the silicate layer.[29,31] Similar observations have been reported by many other researchers based on the organoclay dispersion in PA6 nanocomposites.[1,10] TEM study can provide more detailed dispersion status for OMMT in PA6 nanocomposites.

Scanning electron microscopy. Figures 4(a) to (c) show SEM micrographs of etched fracture surface of ENR-50 toughened PA6 nanocomposites at various ENR-50 concentration. Many dark and/or light pits (holes) and knobs correspond to the ENR-50 particles that proved two-phase morphology, which are clearly visible for all the blends (Figures 4(a) to (c)). These droplets of ENR-50 are dispersed randomly and uniformly within the blends. The range and average particles' size via image analysis data are shown in Table 4. It is obvious from Figure 4 and Table 4 that average particles size of ENR-50 increased with increasing ENR-50 contents (10–30 wt%). The increase in ENR-50 particles size with increased ENR-50 content is attributed to the ENR–ENR interaction in the blends. This is facilitating ENR-50 agglomeration to form large ENR-50 particles, which reduced the aspect ratio of ENR-50 particles. This is the reason why impact strength reduced at 20 and 30 wt% ENR-50 contents. Similarly, previous studies have shown an increase in the rubber particles size by blending rubber in polymer nanocomposites.[10,43] Reduced aspect ratio, rubber size and shape, critical
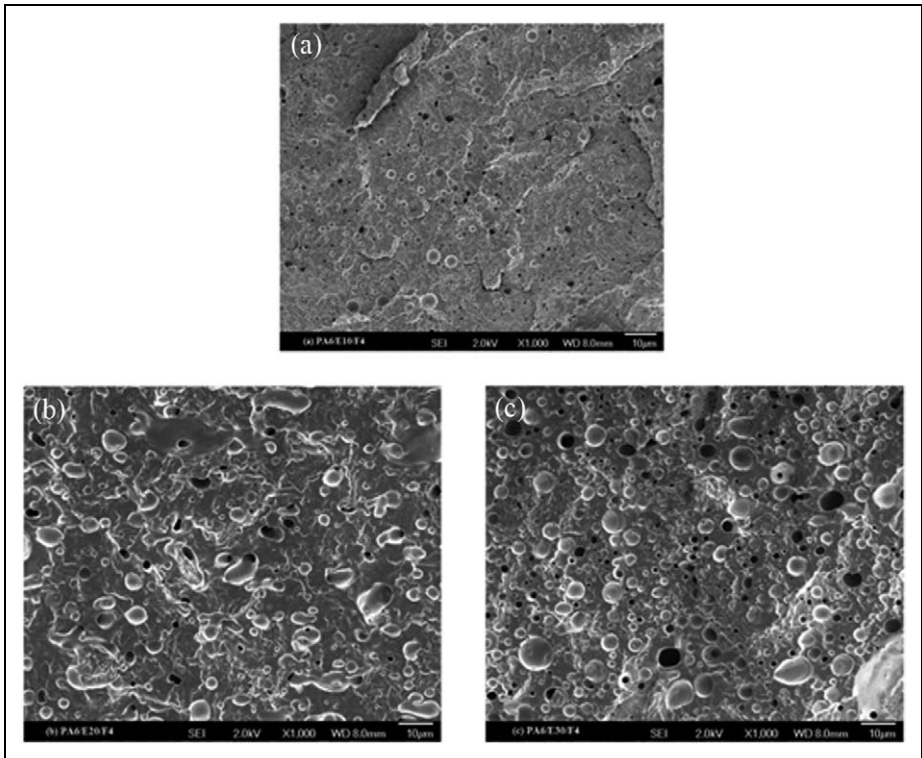
Figure 4. SEM micrograph of cryogenically fractured surfaces of PA6/ENR-50/OMMT ternary blends after etching of ENR-50 with toluene: (a) PA6/E10/F4, (b) PA6/E20/F4 and (c) PA6/E30/F4. PA6: polyamide 6; ENR: epoxidized natural rubber; OMMT: organoclay-modified montmorillonite; SEM: scanning electron microscopy.

Table 4. Range and average of droplet size of ENR-50 particles in PA6 nanocomposites.

Samples	Range of particles size (µm)	Average of particles size (µm)
PA6/E10/F4	0.2–2	0.8
PA6/E20/F4	0.5–6	3
PA6/E30/F4	0.5–8	5

PA6: polyamide 6; ENR: epoxidized natural rubber.

rubber distance and energy absorbance are the important items that influence on the mechanical properties as reported in many studies.[34,40,43,44]

Transmission electron microscopy. The most powerful and direct evidence to describe whether the nanocomposites are exfoliated or intercalated is by the means of TEM.
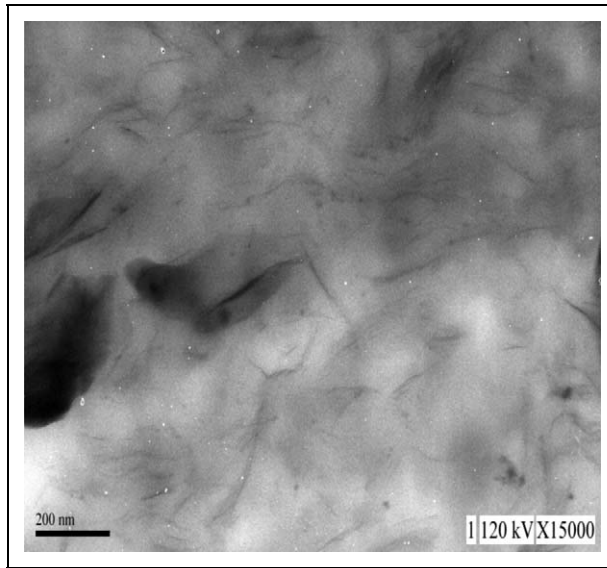
Figure 5. TEM images of exfoliated PA6/ENR-50/OMMT (90/10/4) nanocomposites. PA6: polyamide 6; ENR: epoxidized natural rubber; OMMT: organoclay-modified montmorillonite; TEM: transmission electron microscopy.

Figure 5 shows the TEM micrograph taken from toughened PA6 nanocomposite which consists of 4 phr OMMT. The dark lines represent thickness of the individual clay layers or agglomerates (tactoids and stacks) and the gray part is PA6/ENR-50 blend. Previous researchers observed the exfoliation of OMMT in PA6 and/or ENR-50.[4,29] It is interesting to observe that the OMMT platelets are well dispersed in the PA6/F4/E10 nanocomposites and penetrated or intrude into both PA6 matrix and ENR-50 particles. The well dispersion of OMMT remaining in PA6 matrix and ENR-50 is due to compatibility, which led to miscible blend system results in exfoliation or intercalation structure. Accordingly, the compatibility and strong interaction facilitate the penetration of PA6 and ENR-50 molecules into the OMMT layers' gallery.

Conclusions

The mechanical and thermal properties as well as morphological characterizations of ENR-50 toughened PA6 nanocomposites have been investigated. The impact strength and elongation at break of ternary PA6 nanocomposites increased, while tensile and flexural strength and modulus decreased with increasing ENR-50 content. Maximum toughness was achieved at 10 wt% ENR-50. DSC analysis showed that ENR-50 contents have slightly changed the T_m, T_c and X_c. TGA revealed that the incorporation of ENR-50 reduced the thermal stability of ENR-50 toughened PA6 nanocomposites. SEM analysis showed that ENR-50 particles size increased with an increase in ENR-50 loading and randomly dispersed in PA6 matrix. XRD provided the evidence of exfoliation in

nanocomposites and OMMT platelets were seen to be well-dispersed at ≤ 4 phr in PA6/ENR-50/OMMT nanocomposites, which was confirmed with TEM.

Funding

References

1. Chow WS and Mohd Ishak ZA. Mechanical, morphological and rheological properties of polyamide 6/organo-montmorillonite nanocomposites. *Express Polymer Lett* 2007; 1(2): 77–83.
2. Chavarria F and Paul DR. Comparison of nanocomposites based on nylon 6 and nylon 66. *Polymer* 2004; 45(25): 8501–8515.
3. Wilkinson AN, Man Z, Stanford JL, Matikainen P, Clemens ML, Lees GC, et al. Tensile properties of melt intercalated polyamide 6: montmorillonite nanocomposites. *Compos Sci Tech* 2007; 67(15–16): 3360–3368.
4. Tjong SC. Structural and mechanical properties of polymer nanocomposites. *Mater Sci Eng R: Rep* 2006; 53(3–4): 73–197.
5. Hedicke K, Wittich H, Mehler C, Gruber F and Altstädt V. Crystallisation behaviour of polyamide-6 and polyamide-66 nanocomposites. *Compos Sci Tech* 2006; 66(3–4): 571–575.
6. Baker AMM and Mead J. Thermoplastics. In: Harper CA (ed) *Handbook of plastics, elastomers and composites*, 4th ed. New York, NY: McGraw-Hill, 2002.
7. Donald AM. Failure mechanism in polymeric materials. In: Collyer AA (ed) *Rubber toughened engineering plastics*. 1st ed. London, UK: Chapman and Hall, 1994.
8. Százdi L, Pozsgay A and Pukánszky B. Factors and processes influencing the reinforcing effect of layered silicates in polymer nanocomposites. *Eur Polym J* 2007; 43(2): 345–359.
9. Shishan W, Dingjun J, Xiaodong O, Fen W and Jian S. The structure and properties of pa6/mmt nanocomposites prepared by melt compounding. *Polym Eng Sci* 2004; 44(11): 2070–2074.
10. González I, Eguiazábal JI and Nazábal J. Rubber-toughened polyamide 6/clay nanocomposites. *Compos Sci Tech* 2006; 66(11–12): 1833–1843.
11. Ahn YC and Paul DR. Rubber toughening of nylon 6 nanocomposites. *Polymer* 2006; 47(8): 2830–2838.
12. Bourbigot S, Devaux E and Flambard X. Flammability of polyamide-6/clay hybrid nanocomposite textiles. *Polym Degrad Stabil* 2002; 75(2): 397–402.
13. Kashiwagi T, Harris RH Jr, Zhang X, Briber RM, Cipriano BH, Raghavan SR, et al. Flame retardant mechanism of polyamide 6 clay nanocomposites. *Polymer* 2004; 45(3): 881–891.
14. Russo GM, Nicolais V, Di Maio L, Montesano S and Incarnato L. Rheological and mechanical properties of nylon 6 nanocomposites submitted to reprocessing with single and twin screw extruders. *Polym Degrad Stabil* 2007; 92(10): 1925–1933.
15. Fornes TD and Paul DR. Crystallization behavior of nylon 6 nanocomposites. *Polymer* 2003; 44(14): 3945–3961.
16. Kusmono, Mohd Ishak ZA, Chow WS, and Takeichi T and Rochmadi. Influence of SEBS-*g*-MA on morphology, mechanical, and thermal properties of PA6/PP/organoclay nanocomposites. *Eur Polym J* 2008; 44(4): 1023–1039.
17. Contreras V, Cafiero M, Da Silva S, Rosales C, Perera R and Matos M. Characterization and tensile properties of ternary blends with PA-6 nanocomposites. *Polym Eng Sci* 2006; 46(8): 1111–1120.

18. Baldi F, Bignotti F, Tieghi G and Riccò T. Rubber toughening of polyamide 6/organoclay nanocomposites obtained by melt blending. *J Appl Polym Sci* 2006; 99(6): 3406–3416.

19. Wang K, Wang C, Li J, Su J, Zhang Q, Du R, et al. Effects of clay on phase morphology and mechanical properties in polyamide 6/EPDM-*g*-MA/organoclay ternary nanocomposites. *Polymer* 2007; 48(7): 2144–2154.

20. Hassan A, Wahit MU and Chee CY. Mechanical and morphological properties of PP/NR/LLDPE ternary blend: effect of HVA-2. *Polym Test* 2003; 22(3): 281–290.

21. Mishra S, Sonawane SS and Shimpi NG. Influence of organo-montomorillonite on mechanical and rheological properties of polyamide nanocomposites. *Appl Clay Sci* 2009; 46(2): 222–225.

22. Zhang L, Wan C and Zhang Y. Investigation on morphology and mechanical properties of polyamide 6/maleated ethylene-propylene-diene rubber/organoclay composites. *Polym Eng Sci* 2009; 49(2): 209–216.

23. Kelnar I, Khunová V, Kotek J and Kaprálková L. Effect of clay treatment on structure and mechanical behavior of elastomer-containing polyamide 6 nanocomposite. *Polymer* 2007; 48(18): 5332–5339.

24. Lim JW, Hassan A, Rahmat AR and Wahit MU. Morphology, thermal and mechanical behavior of polypropylene nanocomposites toughened with poly(ethylene-co-octene). *Polymer Int* 2006; 55(2): 204–215.

25. González I, Eguiazábal JI and Nazábal J. Compatibilization level effects on the structure and mechanical properties of rubber-modified polyamide-6/clay nanocomposites. *J Polym Sci B: Polym Phys* 2005; 43(24): 3611–3620.

26. Wu G, Xu H and Zhou T. Morphology evolution, crystalline orientation, and thermal expansion of PA6/SEBS blends with nanolayer networks. *Polymer* 2010; 51(15): 3560–3567.

27. Yoksan R. Epoxidized natural rubber for adhesive applications. *Kasetsart J* (Natural Science) 2008; 42: 325–332.

28. Gelling IR. Epoxidised natural rubber. *J Nat Rubber Res* 1991; 6(3): 184–205.

29. Varghese S, Karger-Kocsis J and Gatos KG. Melt compounded epoxidized natural rubber/layered silicate nanocomposites: structure-properties relationships. *Polymer* 2003; 44(14): 3977–3983.

30. Xie BH, Yang MB, Li SD, Li ZM and Feng JM. Studies on polyamide-6/polyolefin blend system compatibilized with epoxidized natural rubber. *J Appl Polym Sci* 2003; 88(2): 398–403.

31. Nematzadeh N, Wahit MU, Hassan A and Mahmoudian S. Mechanical and thermal properties of polyamide 6 nanocomposites toughened with epoxidized natural rubber-25. *Key Eng Mater* 2011; 471–472: 518–523.

32. Utracki LA. Clay-containing polymeric nanocomposites vol 1. Shawbury, UK: Rapra Technology Limited, 2004.

33. Wahit MU, Hassan A, Mohd Ishak ZA and Abu Bakar A. The effect of polyethylene-octene elastomer on the morphological and mechanical properties of polyamide 6/polypropylene nanocomposites. *Polym Polym Compos* 2005; 13(8): 795–806.

34. Tanrattanakul V, Sungthong N and Raksa P. Rubber toughening of nylon 6 with epoxidized natural rubber. *Polym Test* 2008; 27(7): 794–800.

35. Wahit MU, Hassan A, Koay YF, Othman N and Mokhtar M. Toughening of polyamide 6 nanocomposites: effect of organoclay and maleic anhydride grafted polyethylene octene loading on morphology and mechanical properties. *Int J Mech Mater Eng* 2009; 4(1): 76–87.

36. Dasari A, Yu ZZ, Yang M, Zhang QX, Xie XL and Mai YW. Micro and nano-scale deformation behavior of nylon 66-based binary and ternary nanocomposites. *Compos Sci Tech* 2006; 66(16): 3097–3114.

37. Teh PL, Mohd Ishak ZA, Hashim AS, Karger-Kocsis J and Ishiaku US. Effects of epoxidized natural rubber as a compatibilizer in melt compounded natural rubber organoclay nanocomposites. *Eur Polym J* 2004; 40(11): 2513–2521.

38. Laura DM, Keskkula H, Barlow JW and Paul DR. Effect of rubber particle size and rubber type on the mechanical properties of glass fiber reinforced, rubber-toughened nylon 6. *Polymer* 2003; 44(11): 3347–3361.

39. Souheng W. Phase structure and adhesion in polymer blends: a criterion for rubber toughening. *Polymer* 1985; 26(12): 1855–1863.

40. Wang XH, Zhang HX, Jiang W, Wang ZG, Liu CH, Liang HJ, et al. Toughening of nylon with epoxidised ethylene propylene diene rubber. *Polymer* 1998; 39(12): 2697–2699.

41. Othman N, Azman H, Rahmat AR and Wahit MU. Preparation and characterisation of polyethylene-octene grafted maleic anhydride-toughened 70:30 PA6/PP/MMT nanocomposites. *Polym Polym Compos* 2007; 15: 217–227.

42. Zurina M, Ismail H and Ratnam CT. The effect of HVA-2 on properties of irradiated epoxidized natural rubber (ENR-50), ethylene vinyl acetate (EVA), and ENR-50/EVA blend. *Polym Test* 2008; 27(4): 480–490.

43. Lim JW, Hassan A, Rahmat AR and Wahit MU. Rubber-toughened polypropylene nanocomposite: effect of polyethylene octene copolymer on mechanical properties and phase morphology. *J Appl Polym Sci* 2006; 99(6): 3441–3450.

44. Balakrishnan H, Hassan A and Wahit MU. Mechanical, thermal, and morphological properties of polylactic acid/linear low density polyethylene blends. *J Elastomers Plast* 2010; 42: 223–239.